communications earth & environment

Article

https://doi.org/10.1038/s43247-024-01569-3

Seafloor alkalinity enhancement as a carbon dioxide removal strategy in the Baltic Sea

Andrew W. Dale[1] ✉, Sonja Geilert[1,2], Isabel Diercks[1], Michael Fuhr[1], Mirjam Perner[1], Florian Scholz[1,3] & Klaus Wallmann[1]

Carbon dioxide removal from the atmosphere and storage over long times scales in terrestrial and marine reservoirs is urgently needed to limit global warming and for sustainable management of the global carbon cycle. Ocean alkalinity enhancement by the artificial addition of carbonate minerals to the seafloor has been proposed as a method to sequester atmospheric CO_2 and store it in the ocean as dissolved bicarbonate. Here, a reaction-transport model is used to scrutinize the efficacy of calcite addition and dissolution at a well-studied site in the southwestern Baltic Sea – a brackish coastal water body in northern Europe. We find that most calcite is simply buried without dissolution under moderate addition rates. Applying the model to other sites in the Baltic Sea suggests that dissolution rates and efficiencies are higher in areas with low salinity and undersaturated bottom waters. A simple box model predicts a tentative net CO_2 uptake rate from the atmosphere of 3.2 megatonnes of carbon dioxide per year for the wider Baltic Sea after continually adding calcite to muddy sediments for 10 years. More robust estimates now require validation by field studies.

The Intergovernmental Panel on Climate Change's special report on the impacts of global warming of 1.5 °C above pre-industrial levels concluded that additional interventions aside from reduced carbon dioxide (CO_2) emissions and transition to renewable energy sources will be needed to avoid exceeding this threshold[1]. One such intervention, pro-active carbon dioxide removal (CDR) from the atmosphere and storage over long times scales, may help to mitigate climate change. Conventional CDR approaches are primarily land-based and currently sequester around 2 Gt of CO_2 per year, mostly via afforestation, reforestation and forest management[2]. Until now, novel CDR approaches such as biochar, direct air carbon capture and storage and marine-based approaches amount to only a tiny fraction of conventional CDR (0.002 Gt of CO_2) as they are mostly still in trial phases[2]. Yet, they must be scaled up rapidly by several orders of magnitude to meet the Paris Agreement temperature goal, and the number of scientific investigations in these areas is growing rapidly[2,3].

The oceans have currently absorbed about half of historical anthropogenic CO_2 emissions, resulting in an increase in dissolved CO_2 concentrations and a decline in the pH of surface ocean waters[4]. Consequently, along with ocean warming, their capacity to absorb ever-more CO_2 is decreasing over time[5]. The efficiency of CO_2 uptake could be increased by ocean alkalinity enhancement (OAE), which entails adding mineral alkalinity or chemical bases to seawater to convert CO_2 to dissolved bicarbonate (HCO_3^-) and thereby enhance CO_2 uptake from the atmosphere to restore equilibrium, or slow down CO_2 release in areas of CO_2 outgassing[3]. Alkalinity enhancement essentially represents an acceleration of natural weathering of rocks on land; a process that is currently too slow to fully compensate for man-made residual CO_2 emissions. OAE is one of several novel CDR methods noted for its high potential for mitigation effectiveness against global warming and ocean acidification[2,6]. The true potential of OAE for large-scale deployment is not clear[6–8], although it is thought to be capable of sequestering $3 - 30$ Gt CO_2 yr^{-1} [6,9,10]. This uncertainty is partly due to a lack of clear understanding concerning the marine regions best suited to achieve the greatest possible benefit of OAE[8].

Using a state-of-the-art reaction-transport model, this study investigates the targeted input of carbonate minerals to fine-grained sediments on the seafloor. We chose to investigate carbonate rather than mafic minerals such as olivine since experiments have shown that the rate of dissolution of carbonates is faster[11]. In muddy sediments, the natural degradation of particulate organic carbon (POC) combined with the aerobic oxidation of reduced metabolites such as hydrogen sulphide produces protons close to the sediment surface and a shift in carbonate system toward lower pH (i.e. higher porewater CO_2 concentrations)[12]. These oxidation processes are

[1]GEOMAR Helmholtz Centre for Ocean Research Kiel, Wischhofstr. 1–3, 24148 Kiel, Germany. [2]Present address: Department of Earth Sciences, Utrecht University, Utrecht, The Netherlands. [3]Present address: Institute for Geology, Center for Earth System Research and Sustainability, Universität Hamburg, Hamburg, Germany. ✉e-mail: adale@geomar.de

often associated with a thin subsurface layer that is undersaturated with respect to carbonate minerals ($CaCO_3$), allowing dissolution and partial neuralization of the ambient acidity[12] (Fig. 1):

$$CaCO_3 + CO_2 + H_2O = > Ca^{2+} + 2HCO_3^- \quad (1)$$

The reaction increases alkalinity by the production of one mole of divalent calcium ions (Ca^{2+}) or 2 moles of mono-valent HCO_3^-. The coupling between POC degradation and mineral dissolution has been termed the 'benthic weathering engine'[13,14] and enhances the benthic flux of total alkalinity (TA) to the water column. For calcite dissolution, the TA and DIC fluxes increase in a 2:1 ratio, raising the pH in the water column and lowering the partial pressure of CO_2[15]. Subsequent equilibration of the carbonate system will sequester CO_2 from the atmosphere to restore atmospheric CO_2 partial pressure in the water column.

Our study area is the 28 m deep Boknis Eck basin, Eckernförde Bight, in the German sector of the SW Baltic Sea (54°31.77N, 10°02.36E). The Baltic Sea is a promising location for benthic OAE because it displays a low natural alkalinity due to its brackish waters, with a pronounced salinity gradient along its major axis. Sluggish mixing during late summer at Boknis Eck drives bottom water hypoxia or even anoxia, as well as low pH and undersaturation with respect to biogenic carbonate, which should further promote carbonate dissolution[16]. Hence, in some ways, Boknis Eck resembles other larger seasonally hypoxic or permanently anoxic regions in the Baltic Sea that have become more extensive and oxygen-depleted in recent decades[17]. A wealth of benthic biogeochemical data is available for Boknis Eck, which has been the focus of regular monitoring of water column biogeochemistry and physical parameters since the 1950s[16,18], including periods where TA and pH were measured[16]. Extensive analysis of sediment biogeochemistry has also been accomplished[19–21]. We use this information to help constrain model simulations for Boknis Eck sediment biogeochemistry and the impact of artificial carbonate addition. We then adapt the model to assess rates of carbonate dissolution in other regions of the Baltic Sea, displaying pronounced differences in bottom water O_2, pH, and salinity. Finally, using a simple box model of the water column representative of several regions of the Baltic Sea, we then discuss the wider feasibility of benthic OAE as a potential CDR strategy.

Results and discussion

Background seasonal conditions

To begin with, we use the 1-D reaction-transport model to explore the seasonality of the sediment biogeochemistry at Boknis Eck without artificial calcite addition (see Methods). The model accounts for aerobic and anaerobic degradation of organic carbon in addition to a variety of secondary redox reactions (Supplementary Tables 1–4). The model is forced using observed seasonal trends in bottom water S, T, pH and dissolved O_2, as well as POC and $CaCO_3$ fluxes to the seafloor (see Methods and Supplementary Fig. 1). The POC rain rate of 12 mmol m^{-2} d^{-1} has been determined previously[20]. The natural input of calcite (2.9 mmol m^{-2} d^{-1}) due to coastal and seabed erosion is adjusted to provide observed average carbonate contents in the sediment column of around 3–4 wt.%[22]. The simulated solid phase and dissolved species in the sediment are in good agreement with available observations (see Supplementary Fig. 2).

The model shows that the simulated redox conditions in the sediment, pH, and rate of calcite dissolution at Boknis Eck prior to artificial calcite addition are strongly governed by the seasonal variability in oxygen concentration in the ambient bottom water that varies from ~350 µM in winter and spring to near-anoxia in late summer (Fig. 2). In winter, oxygen penetrates several mm into the sediment by diffusion and bio-irrigation (Fig. 2 and Supplementary Fig. 3). Porewater pH in the top cm is lowest when oxygen is present due to the acidity generated by aerobic sulphide, iron and ammonium oxidation, despite the fact that bottom water pH is found at its maximum level (Supplementary Fig. 1). The sediment layer thickness where pore fluids are undersaturated with respect to calcite ($\Omega_{Calcite}$ <1) oscillates between ca. 1.3 cm in winter/spring and 0.4 cm in summer/autumn (Supplementary Fig. 3C). This drives a clear seasonality in calcite dissolution. Maximum rates are observed at the sediment surface in summer/autumn when the deposited calcite is bathed in undersaturated, low-oxygen bottom waters. In winter, calcite dissolution migrates downwards to subsurface layers (~5 mm) where dissolution is driven by aerobic respiratory pathways, i.e. the benthic weathering engine (Fig. 3f). As a result, seasonal changes in porewater buffering become apparent, as shown by the sensitivity of pH to changes in TA, $\partial pH/\partial TA$[15] (Supplementary Fig. 3). Apparently, therefore, the benthic weathering engine, linked to the availability of oxygen, in addition to the calcite saturation state of the bottom water are both important for (natural) calcite dissolution at Boknis Eck.

Mean annual rates of calcite dissolution (R_{CaDiss}) are 0.97 mmol m^{-2} d^{-1}, with benthic TA and DIC fluxes to the bottom water of 10.1 and 12.9 mmol m^{-2} d^{-1}, respectively (Fig. 3a, b). TA and DIC fluxes are much larger than R_{CaDiss} due to high rates of POC degradation (12 mmol m^{-2} d^{-1}) that mostly occurs anaerobically by sulphate reduction. Sulphate reduction is by far the most important alkalinity-producing reaction at Boknis Eck (Table 1). Most of the sulphide produced by sulphate reduction is precipitated and buried as iron mineral phases that accumulate to high levels of 2–3 wt. %, similar to the anoxic Gotland Basin in the eastern Baltic Sea[23] (Supplementary Fig. 2). High S burial in these systems might be caused by shuttling of reactive particulate iron from shallower to deeper waters and subsequent binding of reduced S[24–27]. Burial of sulphide represents a major source of alkalinity at Boknis Eck, accounting for around three-quarters of the net TA flux (Table 1). Consequently, the TA:DIC flux ratio of 0.78 is well-below the theoretical value of two expected for calcite dissolution (Eq. (1)), and more similar to the 1:1 ratio for sulphate reduction (Fig. 4c, Supplementary Table 1).

The respiratory index (RI), defined here as the ratio of R_{CaDiss} to POC degradation, indicates that only 8% of the CO_2 released during POC degradation is neutralized by calcite dissolution and converted into alkalinity (Fig. 3d). In the current model configuration, the rather low calcite dissolution efficiency (dissolution rate/calcite added) of 30% allows most

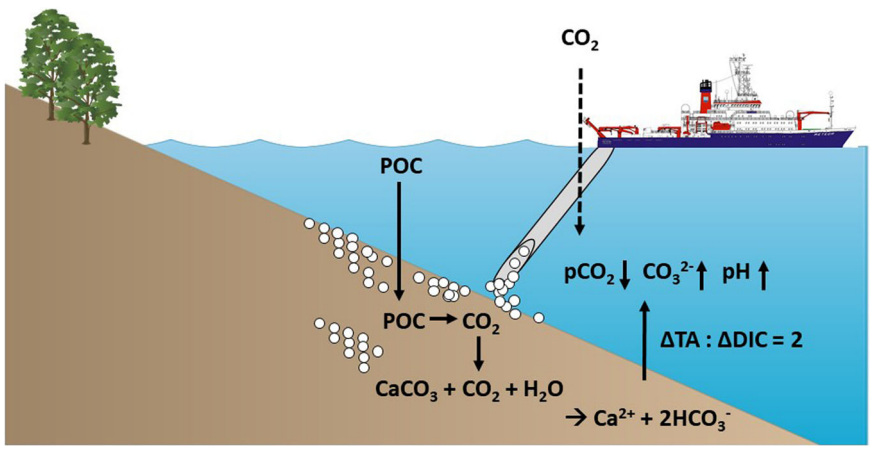

Fig. 1 | Ocean alkalinity enhancement through benthic carbonate dissolution. Photosynthetically-derived particulate organic carbon (POC) sinks from surface waters to the seafloor, whereupon it is respired by microorganisms to CO_2, leading to undersaturation of sediment porewaters with respect to carbonate minerals[28,56]. A fraction of the metabolic CO_2 is consumed during the dissolution of calcium carbonate artificially added to the seafloor (white circles). This results in a flux of alkalinity and DIC to the water column in a 2:1 ratio, thereby raising the pH and lowering the partial pressure of CO_2[15]. Equilibration with the atmosphere will produce the envisioned CO_2 uptake from the atmosphere to the water column (dashed arrow).

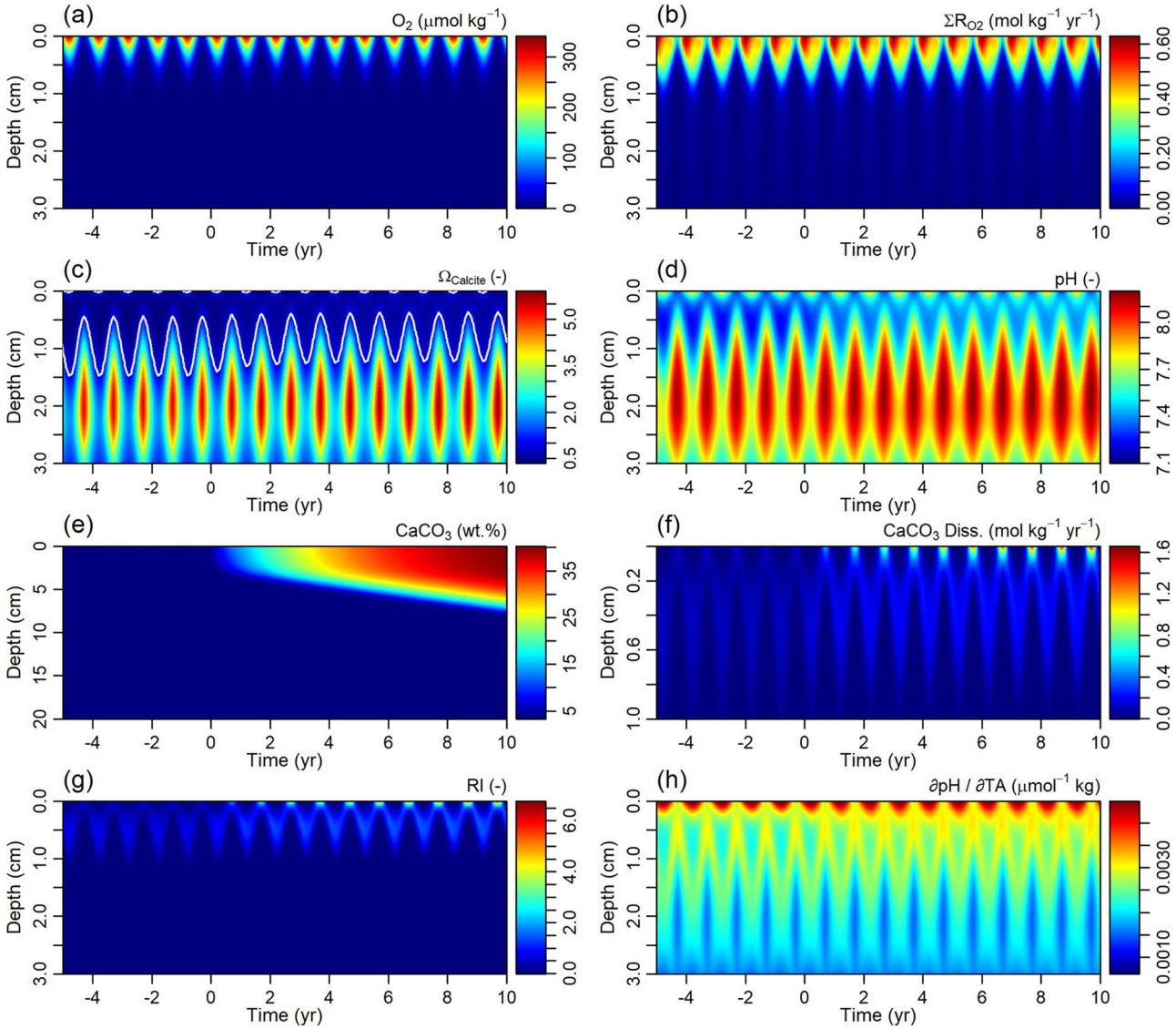

Fig. 2 | Modelled benthic biogeochemistry in surface sediments of Boknis Eck. **a** O_2 concentration, **b** total rate of oxygen consumption, **c** calcite saturation state, **d** pH, **e** calcite content, **f** calcite dissolution rate, **g** respiratory index (carbonate dissolution ÷ POC degradation), **h** sensitivity factor of pH to changes in TA. The white line in (**c**) denotes $\Omega_{Calcite} = 1$. The x-axis shows time in years relative to artificial calcite addition beginning at year zero (24 mmol m^{-2} d^{-1}). Calendar years begin on 1 January. Note the different depth scales for $CaCO_3$ and calcite dissolution. High temporal resolution plots are shown in the Supplementary Material.

calcite to be buried below the thin undersaturated surface layer. Thus, despite the fact that POC rain rates are four-fold higher than natural calcite fluxes, calcite dissolution under natural conditions at Boknis Eck is inherently inefficient. This is partially explained by the brief time that calcite resides in the thin undersaturated layer. Downward mixing of particles by bioturbation to depths where dissolution is thermodynamically inhibited helps to preserve calcite. Calcite dissolution rates can be increased by the presence of cable bacteria performing electrogenic sulphide oxidation[13,14]. This enigmatic oxidation pathway produces protons in a 1–2 cm thick layer below the sediment surface and leads to strong undersaturation with respect to calcite[28,29]. Cable bacteria were not included in the model since their presence in incubated sediments from Boknis Eck seems to be rather ephemeral in nature and not well understood at the present time[30].

Benthic OAE by calcite addition

In a second model scenario, we investigated continuous artificial calcite addition at Boknis Eck over a time period of 10 years at a rate of 24 mmol m^{-2} d^{-1} (twice the annual rain rate of POC, see Methods). The results follow similar trends as before, with a greater extent of undersaturated porewaters with respect to calcite during winter and spring when oxygen is available, whereas oversaturation prevails in the late summer when oxygen is depleted (Fig. 2 and Supplementary Fig. 3). Calcite dissolution increases sharply following mineral addition, and after ca. 10 years approaches a new steady state of 2.6 mmol m^{-2} d^{-1} (Fig. 3a). TA and DIC fluxes increase to 13.4 and 14.5 mmol m^{-2} d^{-1}, respectively, with a modest increase in the TA:DIC flux ratio to 0.92. The corresponding drop in the benthic CO_2 flux from 2.2 to 0.95 mmol m^{-2} d^{-1} demonstrates that the artificial addition of calcite neutralizes porewater CO_2 and leads to a decrease in benthic CO_2 emissions (Fig. 3b). The self-buffering of the porewater by the additional alkalinity supplied by the dissolving calcite leads to a narrowing over time of the zone where porewaters are undersaturated with respect to calcite and thus a plateauing of the dissolution rate (Figs. 2c and 3). Surface rates of calcite dissolution during the autumn undersaturated period are ten-fold higher than the natural condition (c.f. Supplementary Figs. 3f and 4f). Nonetheless, and although the RI increases to 22%, most added calcite accumulates in the sediment without further

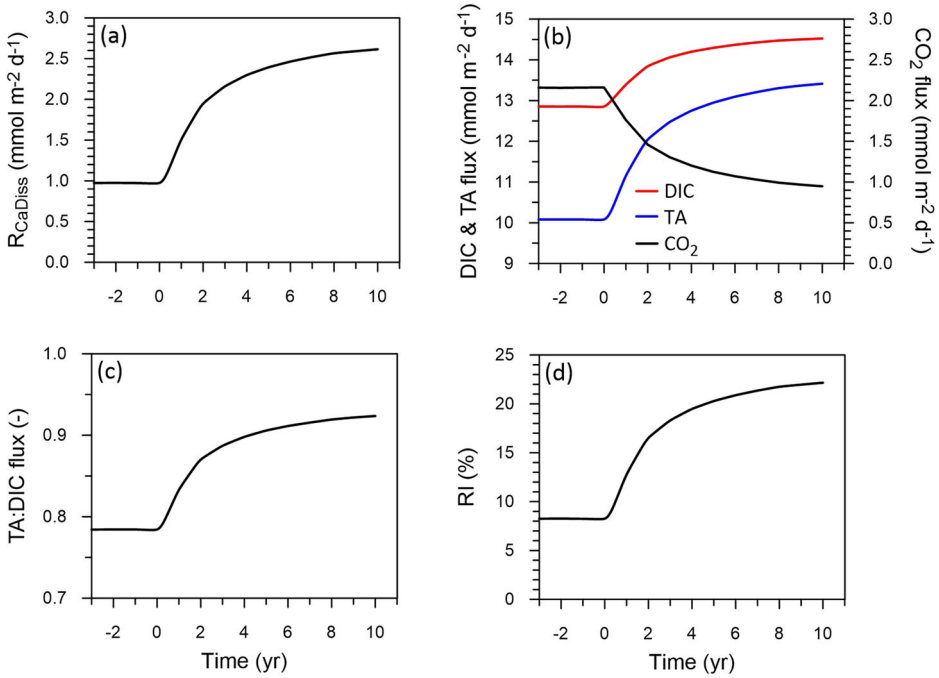

Fig. 3 | Modelled rates and fluxes for Boknis Eck sediments. a Total calcite dissolution rate, **b** benthic fluxes of DIC, TA and CO_2 from the sediment to the bottom water, **c** TA:DIC flux ratio, and (**d**) the respiratory index, RI (carbonate dissolution ÷ POC degradation × 100%) versus time in years relative to the start of artificial calcite addition beginning year zero.

reaction. After ten years of continuous addition, the calcite content at the sediment surface reaches 37%; levels that would, in reality, completely alter the physical and geochemical characteristics of the sediment matrix (Fig. 2e). The impact on benthic fauna associated with the addition of alkaline minerals has received very little attention to date[31].

Further model tests show that the calcite dissolution efficiency decreases with increasing amounts of added calcite (Fig. 4). Highest dissolution efficiencies of >30% are associated with minimal calcite addition (0.5 mmol m^{-2} d^{-1}), yet also with the lowest dissolution rates. This dynamic, which is partly due to the thin subsurface undersaturated layer that throttles complete calcite dissolution, demonstrates that desirable high dissolution rates come at the expense of low dissolution efficiency. The undissolved calcite fraction is simply buried and therefore of no further benefit to CDR. Such considerations would be critical in cost-benefit analyses for upscaling of benthic OAE by alkaline mineral dispersal on the seafloor. It is currently unclear whether the artificial addition of mafic minerals, such as olivine, that are generally far below saturation in marine porewaters, would encounter similar bottlenecks to dissolution[32].

Calcite dissolution in other regions of the Baltic Sea

Based on the above findings, a factorial sensitivity analysis was performed to provide insight into which type of marine environment would be most conducive for benthic calcite dissolution in the wider Baltic Sea region (see Methods). The parameters tested cover typical ranges of pH, O_2, T, S and POC rain rate encountered in the Baltic Sea. The results of the sensitivity analysis demonstrate that bottom water salinity, O_2, and to a lesser extent, pH and POC rain rate are important factors with regard to calcite dissolution (Supplementary Fig. 5A). Dissolution is favoured by low pH and low salinity since they are associated with lower carbonate (CO_3^{2-}) and Ca^{2+} concentrations, respectively, which directly impacts $\Omega_{Calcite}$ (Eq. (3)). High O_2 concentrations and POC availability favour dissolution since aerobic respiratory pathways consume alkalinity and therefore decrease CO_3^{2-} concentrations (i.e. the benthic weathering engine). Temperature emerges as a minor driver for calcite dissolution. To illustrate this point further, the fraction of calcite dissolved at Boknis Eck shows a significant logarithmic relationship with bottom water O_2 concentrations and $\Omega_{Calcite}$ (Supplementary Fig. 5B). Although this relationship simplifies a great deal of biogeochemical complexity, it implies that sediments underlying fully oxygenated and under-saturated bottom waters, or a trade-off thereof, could be candidate locations for benthic OAE applications in the Baltic Sea. Bench-top incubations of Boknis Eck sediment amended with ground-down calcite suggest that $\Omega_{Calcite}$ may be more important than O_2 concentrations in the initial weeks after calcite addition[11,30].

The model boundary conditions were modified to explore calcite dissolution in other environments of the Baltic Sea that display a wide range of O_2, pH and salinity. We examined specific environments in the eastern Gotland Basin (GB) and Bothnian Bay (BB) (Supplementary Table 5). BB is located in the low salinity (~3) region of the northern Baltic Sea, with oxygenated bottom waters (~300 µM) and fine-grained muddy sediment away from the coastline[33,34]. BB bottom waters are strongly undersaturated with respect to calcite ($\Omega_{Calcite}$ ~0.13, Supplementary Table 5). The bottom waters of GB (250 m deep) are also undersaturated ($\Omega_{Calcite}$ ~0.2) and near-permanently anoxic due to sluggish mixing, with a salinity of ~13[35]. Sediments lying within the depth range where the chemocline impinges the seafloor (80–120 m)[36] are bathed in undersaturated ($\Omega_{Calcite}$ ~0.3 m) and hypoxic (<63 µM O_2) bottom waters. In the shallower, permanently oxic depths above the chemocline (O_2 > 300 µM), bottom water salinity is ~7 and pH is ~8.1, with $\Omega_{Calcite}$ values of ~1.2. The lower pH below the chemocline (7.1) is probably driven by the predominant respiration of organic matter by sulphate reduction that converges to a pH of 6.7[37]. POC rain rates across these four settings range from approximately 3 to 9 mmol m^{-2} d^{-1}. The model boundary conditions to simulate calcite dissolution at these sites are assumed to be constant over time (Supplementary Table 5). Kinetic parameters were unchanged from the Boknis Eck simulation and the model results are not constrained by sediment porewater data or benthic flux measurements due to lack of relevant data. The model also does not include TA sinks by the precipitation of Mn-carbonates that are abundant in GB[38]. Therefore, results from this exercise provide a tentative benchmark for calcite dissolution at these localities compared to Boknis Eck.

Model simulations show that the calcite content in sediments before mineral addition is generally <1%, in agreement with available observations[33] (Supplementary Fig. 6). After 10 yr of calcite addition, carbonate again accumulates in the surface layers, reaching 12% in the anoxic GB, 8% in BB, 10% in the hypoxic GB and 35% in the oxic GB. BB and GB display notably higher rates of calcite dissolution compared to Boknis Eck, with dissolution efficiencies that exceed 50% in BB and the anoxic and

Table 1 | Reaction rates at Boknis Eck and their contribution to TA prior to addition of calcite

	Rate ($\mu mol\ cm^{-2}\ yr^{-1}$)	ΔTA (Supplementary Table S1)	Rate TA ($\mu mol\ cm^{-2}\ yr^{-1}$)	
POC degradation by O_2	82.1	0.14	11.6	
POC degradation by NO_3^-	30.7	0.94	28.9	
POC degradation by SO_4^{2-}	313.6	1.14	358.0	
POC degradation by CH_4	11.2	0.14	1.6	
Aerobic NH_4^+ oxidation	33.2	−2	−66.5	
Anaerobic NH_4^+ oxidation	0.5	−0.67	-0.3	
Aerobic H_2S oxidation	10.7	−2	−21.4	
Aerobic Fe^{2+} oxidation	17.1	−2	−34.2	
Anaerobic H_2S oxidation	5.2	0	0.0	
Pyrite formation	53.3	2	106.6	
Aerobic pyrite oxidation	0.1	−2	−0.2	
FeS precipitation	31.6	−2	−63.2	
FeS dissolution	0.1	2	0.3	
Aerobic FeS oxidation	16.5	−2	−33.1	
Anaerobic CH_4 oxidation	5.5	2	10.9	
$CaCO_3$ dissolution	36.2	2	72.4	
$CaCO_3$ precipitation	0.0	−2	0.0	
TA flux at bottom	4.7	−1	−4.7	
		Sum	366.7	$\mu mol\ cm^{-2}\ yr^{-1}$
		Sum	10.0	$mmol\ m^{-2}\ d^{-1}$
FeS burial	15.5	2	31.1	
FeS_2 burial	53.3	4	213.3	
POC degradation by NO_3^-	30.7	0.94	28.9	
$CaCO_3$ dissolution	36.2	2	72.4	

Also shown are the irreversible TA sources by sulphide burial, denitrification and calcite dissolution. Results after adding calcite are given in Supplementary Table 7.

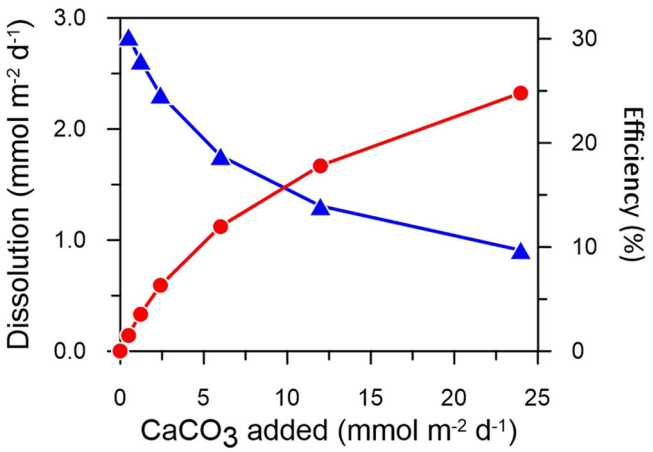

Fig. 4 | Rates and efficiency of artificial calcite dissolution. Calcite dissolution rate (red curve) and dissolution efficiency (blue curve) in Boknis Eck sediments versus the flux of calcite added to the seafloor. Symbols represent individual model runs after 10 years of calcite addition.

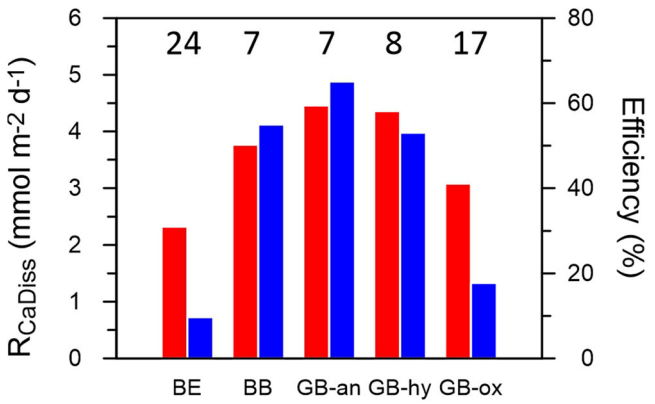

Fig. 5 | Model results for artificial calcite dissolution in other areas of the Baltic Sea. Calcite dissolution (red bars) and dissolution efficiency (blue bars) are shown for Bothnian Bay (BB), and the anoxic, hypoxic and oxic sites of Gotland Basin (GB). Results represent the mean value for year 10 after calcite addition. Calcite addition rates (= 2 × POC rain rate), are given at the top of the figure in $mmol\ m^{-2}\ d^{-1}$. Results for Boknis Eck (BE) are shown for comparison.

hypoxic regions of GB (Fig. 5). Due to limited bioturbation in the poorly oxygenated and undersaturated bottom waters of GB, calcite is able to dissolve on the sediment surface. Like Boknis Eck, a quasi-steady state in calcite dissolution is reached after ~10 yr, at which point BB and the anoxic and hypoxic GB sediments become strong sinks for bottom water dissolved CO_2 (2.5 – 4.5 $mmol\ m^{-2}\ d^{-1}$; Supplementary Fig. 7).

These results, although associated with many uncertainties, support the idea that the eastern and northern Baltic Sea could be ideal test sites for benthic OAE applications. More sophisticated modelling efforts are needed to explore how benthic alkalinity addition is impacted by water column stratification in the Gotland Basin. The median age of deep water in the

Table 2 | The Baltic Sea sub-basins used to derive CO_2 uptake rates from the atmosphere. Salinity, temperature, and TA data were taken from the BALTSEM model (see Methods)

Sub-basin	Area (km^2)	Mud (km^2)	Mean depth (m)	Mean S (-)	Mean T (°C)	TA (µmol kg^{-1})	pH	O_2 (µmol kg^{-1})	$CaCO_3$ added (Mt yr^{-1})	CO_2 uptake (Mt yr^{-1})	$CaCO_3$:CO_2 (t t^{-1})
Kattegat (Katt)	22249	8500	24	26.4	7.7	2049	8.01	314	4.0	0.044	89.5
Danish Straits (DS)	19331	2300	15	16.6	7.4	1806	8.00	337	1.1	0.022	49.5
Baltic Proper (BP)	227568	74300	61	7.9	4.7	1576	7.90	378	34.7	1.524	22.7
Bothnian Sea (BS)	67001	8800	64	5.3	3.4	1261	7.90	401	4.1	0.341	12.0
Bothnian Bay (BB)	36559	13300	40	3.2	3.2	862	7.74	410	6.2	0.935	6.6
Gulf of Riga (GoR)	17509	8700	24	5.6	5.2	1884	8.07	383	4.1	0.120	33.7
Gulf of Finland (GoF)	23729	8800	33	5.7	4.5	1435	7.96	389	4.1	0.239	17.2
								Total	58.2	3.23	

pH (total scale) was derived from TA assuming the equilibrium of the water boxes with the atmosphere (415 µatm). O_2 concentrations denote solubilities at ambient S and T[91]. Seafloor areas are from Gustafsson et al.[27]. The CO_2 uptake corresponds to the rate after 10 years of calcite addition.

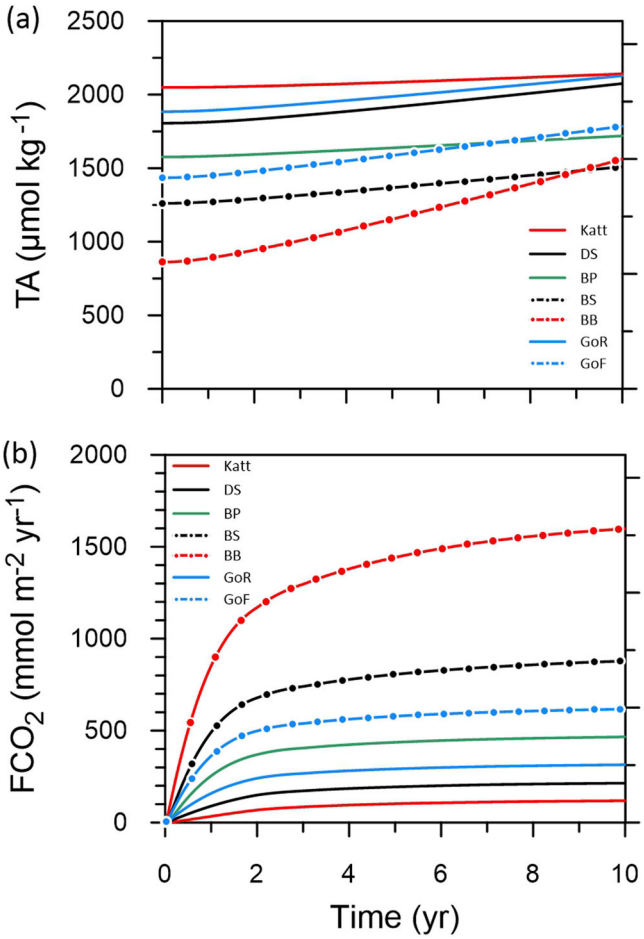

Fig. 6 | Water column box model results. a Total alkalinity, and (**b**) CO_2 uptake from the atmosphere to the water column for the seven sub-basins of the Baltic Sea shown as time after artificial calcite dissolution. The basin abbreviations in the legend are explained in Table 2.

basin is approximately 5 years[39], which imposes a time lag before an acceleration in atmospheric CO_2 uptake can be observed. Our findings, summarized in Fig. 5, highlight the potential for seafloor mineral dissolution in and around the basin, and call for more fieldwork in these settings.

Benthic OAE and CDR potential in the Baltic Sea

Turning to the broader question of benthic OAE as a CDR strategy in the Baltic Sea, the benthic model was run for seven sub-basins of the Baltic Sea as defined in the coupled hydrodynamic-biogeochemical model BALTSEM (Baltic Sea Long-term Large-scale Eutrophication Model[27], see Methods). For each sub-basin, mean physico-chemical properties (water depth, T, S, TA) were extracted from BALTSEM and used as boundary conditions for the sediment model (Table 2). The resulting changes in benthic DIC and TA fluxes during 10 yr of artificial calcite addition were then used as inputs to a 1-box model of the water column for each sub-basin assuming well-mixed conditions. The CO_2 uptake from the atmosphere solely due to the addition of calcite was then calculated (Eq. (9), see Methods).

Results show that alkalinity accumulation and CO_2 uptake fluxes from the atmosphere show similar trends across the Baltic Sea, albeit with large differences in magnitude (Fig. 6). The plateauing of CO_2 uptake in all sub-basins reflects the slowing down of benthic dissolution, as seen for Boknis Eck (c.f. Fig. 3b), rather than a decreased capacity of the water column to absorb CO_2. There is a general pattern of higher CO_2 uptake in Bothnian Bay and Bothnian Sea and lower uptake in the western sub-basins in proximity to the North Sea, such as the Danish Straits and Kattegat. This behavior can be attributed to the properties of the carbonate system,

whereby low salinity waters show a greater efficiency of CO_2 sequestration per mole of Ca^{2+} added compared to high salinity waters[7]. In terms of the mass of mineral added in year 10 (t $CaCO_3$ (t CO_2)$^{-1}$), the uptake efficiency ranges from 6.6 t $CaCO_3$ (t CO_2)$^{-1}$ in Bothnian Bay, where bottom water S, TA and pH are lowest, to 89.5 t $CaCO_3$ (t CO_2)$^{-1}$ in the Kattegat where bottom water S, TA and pH are highest (Table 2). Equivalently, the efficiency per mole of alkalinity added ranges from 0.03 to 0.34 mol CO_2 (mol TA added)$^{-1}$. Direct addition of alkaline solutions to surface are likely to be associated with higher efficiencies (~ 0.8 mol CO_2 (mol TA added)$^{-1}$) due to the immediate impact on the carbonate system, provided that spontaneous carbonate precipitation can be curtailed[40]. This direct OAE method does not face similar drawbacks as sediment applications whereby a fraction of the added alkalinity does not interact with the seawater carbonate system (i.e. it is buried instead).

Upscaling the CO_2 flux to the area of fine-grained muddy sediments predicts that an annual uptake of 3.2 Mt CO_2 yr^{-1} is theoretically possible (Table 2). This is equivalent to current upper-end estimates of annual surface CO_2 uptake in the Baltic Sea[41]. Although the model is a very simplified version of reality, it confirms the previous suggestion that low salinity and undersaturated bottom waters are promising sites for CDR via benthic OAE due to (i) low calcite saturation states and high dissolution efficiencies, and (ii) low salinity waters that sequester greater amounts of atmospheric CO_2. Uptake could be up to 10 Mt CO_2 yr^{-1} if calcite dissolution is equally efficient in sandy sediments that account for around two-thirds of the total seafloor area (Table 2). Furthermore, CO_2 sequestration in the Baltic Sea will be more pronounced than reported here, considering that ground-down minerals are likely to be associated with higher dissolution rates than naturally deposited biogenic carbonate[11]. With this in mind, and also considering the fact that the deep anoxic basins are not explicitly accounted for in this regional analysis, our estimate of 3.2 Mt CO_2 yr^{-1} is likely to be a lower estimate of potential CO_2 uptake.

A carbon dioxide removal rate of 3.2 Mt CO_2 yr^{-1} is about the same as current global estimates of CDR by all novel approaches (0.002 Gt), including direct air capture with carbon storage (DACCS) and bioenergy with carbon capture and storage (BECCS)[2]. Storage of atmospheric CO_2 as dissolved bicarbonate in seawater would contribute toward the European Union's goal of reaching net-zero by 2050[42]. The financial costs of widespread deployment may be substantial[2], however, and would need to reflect the fact that the optimal mineral dosage is highly likely to be specific to the local environmental characteristics (Fig. 4)[43]. Monitoring and verification of benthic OAE will also remain challenging in the near future due to the large background seawater alkalinity concentrations and relatively slow rates of calcite dissolution compared to water column mixing and gaseous CO_2 equilibration times[43,44]. Leaving aside the economic, social and legal aspects of OAE in the Baltic Sea, the artificial addition of calcite may be nonetheless be a preferable alternative to mafic silicate minerals such as olivine. Dissolution of these minerals is associated with unwanted side effects, such as release of potentially toxic trace metals and the precipitation of secondary phases (ferric iron oxides and hydroxides, amorphous silica) that diminish rate of net TA production[31,45]. Furthermore, the release of Ca^{2+} and alkalinity by dissolving carbonate minerals may induce precipitation of authigenic phosphate minerals in the sediment[46], and thus help to alleviate ongoing ecological problems in the Baltic Sea such as eutrophication[47], deoxygenation[17] and acidification[48].

Methods

Biogeochemical reaction transport model

The model builds on previous versions that simulate benthic biogeochemistry in the upper 20 cm of sediment[20,21]. Solids include highly reactive (i.e. poorly crystalline) iron (oxyhydr)oxide ($Fe(OH)_3$), crystalline iron (oxyhydr)oxide (Fe_{MR}), iron mono-sulphide (FeS), pyrite (FeS_2), and calcite ($CaCO_3$). The iron phases included in the model are intended to broadly represent the operationally defined fractions from sequential extractions on sediments from Boknis Eck[24]. Solutes include oxygen (O_2), nitrate (NO_3^-), biologically stored nitrate in large sulphur bacteria (bNO_3^-), sulphate (SO_4^{2-}), ferrous iron (Fe^{2+}), total hydrogen sulphide (TH_2S), dissolved inorganic carbon (DIC), protons (H^+), total boron (TB), total ammonia (TNH_3), total phosphate (TPO_4), hydroxyl anion (OH^-), calcium (Ca^{2+}) and methane (CH_4). Solutes and solids are transported by advective and diffusive processes.

The core of the model is the aerobic and anaerobic degradation of organic matter and the subsequent re-oxidation of reduced compounds, including dissolved ammonium, ferrous iron and sulphide. Authigenic pyrite and iron mono-sulphide are further substrates for aerobic oxidation. The oxidation reactions produce protons and drive the dissolution of calcite. The model considers sediment burial, compaction, bioturbation, bioirrigation and biological nitrate transport by sulphide-oxidizing bacteria *Beggiatoa*[20]. Bioirrigation and bioturbation are dependent on bottom water oxygen. A coupled set of mass balance equations (partial differential equations) is set up to simulate the reactive transport of solids and dissolved species (Supplementary Material). Boundary conditions at the sediment surface were defined as fluxes for solids and concentrations for solutes. At the lower model boundary, a zero-gradient condition was used for all species. The model was set up in MATHEMATICA v12 software and solved using finite differences and the method-of-lines. The vertical depth resolution increased from sub-mm scale at the surface to sub-cm scale at depth over a total of 150 grid layers. Mass balance was better than 99.99%.

To define background conditions prior to mineral addition, the model was run into a dynamic (seasonal) steady state representative of the average biogeochemical condition of Boknis Eck sediments (see Supplementary Fig. 2). Porewater data collected quasi-monthly between January 2022 and March 2023 were used to help constrain the model reaction rates, along with particulate iron species. Measured seasonal changes in bottom water dissolved oxygen, pH, salinity, and temperature were used as model forcings at the sediment surface[16]. Concentrations of sulphate, calcium and TA were scaled to salinity. Concentrations of other solutes were fixed at reasonable values for Boknis Eck[20]. The rain rate of calcite to the seafloor was adjusted to simulate observed mean carbonate contents of around 3 – 4 wt.%[22]. The rain rate of particulate organic carbon (POC) was not varied over time due to the uncertainties associated with seasonal POC degradation[20].

Ten years before the end of the model simulation, artificial calcite was added to the sediment surface at a constant rate equal to twice the annual molar rain rate of POC (24 mmol m^{-2} d^{-1} of $CaCO_3$). This flux was chosen on the assumption that it ought to be sufficient to neutralize the carbon dioxide released from the remineralization of organic matter (Fig. 1) and also to limit the neutralization of porewater CO_2 by bottom water CO_3 [49]. To simulate the dissolution of calcite added to the seafloor (Eq. 1), the dissolution rate of calcite (R_{CaDiss} in g g^{-1} yr^{-1}) was calculated applying the following rate law previously used to simulate calcite dissolution in marine sediments[50]:

$$R_{CaDiss} = f_T \cdot k_{CaDiss} \cdot CaCO_3 \cdot \left(1 - \Omega_{Calcite}\right)^{nc} \quad (2)$$

where k_{CaDiss} is a first-order kinetic constant, $\Omega_{Calcite}$ is the saturation state of the pore water with respect to calcite, nc is the reaction order, and the function f_T describes the temperature sensitivity of dissolution (see Supplementary Material). $\Omega_{Calcite}$ was defined as:

$$\Omega_{Calcite} = \frac{\left[Ca^{2+}\right] \cdot \left[CO_3^{2-}\right]}{K_{sp}} \quad (3)$$

$[Ca^{2+}]$, $[CO_3^{2-}]$ and K_{sp} are the porewater concentrations of calcium and carbonate ions, and the solubility constant of calcite, respectively[51]. The solubility constant[52] is based on reagent grade calcium carbonate yet is similar to constants derived from experiments with mixed assemblages of pelagic foraminiferal tests (T = 25 °C, S = 35). It is also the one used in most biogeochemical models and recommended by Zeebe and Wolf-Gladrow[51]. Note that we do not include Mg-carbonate phases that dissolve more rapidly than calcite. Hence, addition of high Mg-carbonate phases may yield higher CO_2 consumption rates when added to seafloor sediments.

Laboratory and field experiments show that the mechanism of carbonate dissolution, and the dissolution rate, depend on solution saturation state[53,54]. Following these studies, and recent modelling of calcite dissolution in deep-sea marine sediments[50], nc and k_{CaDiss} were defined according to two separate regions of the 1 - $\Omega_{Calcite}$ spectrum. For $0.8 < \Omega_{Calcite} < 1$, nc and k_{CaDiss} were 0.8 and 6.3×10^{-3} yr^{-1}, respectively. For $\Omega_{Calcite} \leq 0.8$, nc and k_{CaDiss} were defined as 4.7 and 10 yr^{-1}, respectively, which affords high rates of dissolution when porewaters are far from equilibrium. These constants are lower than those determined from recent short-term (~20 days) sediment core incubations with ground-down calcite added as a large initial pulse[11]. Whilst the present results are more representative of long-term situation that account for slow mixing and burial to oversaturated sediment layers, we acknowledge that calcite dissolution rates immediately following addition may be higher. Fieldwork is planned in the framework of the German research mission CDRmare to quantify this more accurately[55]. Calcite dissolution rates may be slowed by dissolved organic carbon[54] or by secondary mineral precipitation[45,56]. These processes were not considered in the model. Abiotic calcite precipitation was not considered in the model since it is considered to be of relatively limited importance in near-surface marine sediments[12].

pH simulation

Equilibrium processes in the model are applied to DIC ($CO_2 + HCO_3^- + CO_3^{2-}$), TH_2S ($H_2S + HS^-$), water dissociation ($H^+ + OH^-$), TB ($B(OH)_3 + B(OH)_4^-$), TNH_3 ($NH_3 + NH_4^+$), and TPO_4 ($H_3PO_4 + H_2PO_4^- + HPO_4^{2-} + PO_4^{3-}$). We used the direct substitution method of Hoffmann et al.[57] to simulate pH in sediment porewaters. The approach relies on TA as the equilibrium invariant and implicit differential variable to solve for the concentration of protons. TA was defined following Dickson[58], that is, the number of moles of hydrogen ion equivalent to the excess of proton acceptors (bases formed from weak acids with a dissociation constant $K \leq 10^{-4.5}$ at 25 °C and zero ionic strength) over proton donors (acids with $K > 10^{-4.5}$) in 1 kilogram of sample:

$$\begin{aligned} TA = {} & [HCO_3^-] + 2[CO_3^{2-}] + [B(OH)_4^-] + [HS^-] + [NH_3] \\ & + [HPO_4^-] + 2[PO_4^{2-}] + [OH^-] - [H_3PO_4^-] - [H^+] \end{aligned} \quad (4)$$

Minor species that do not contribute substantially to porewater buffering over typical pH ranges of sediment porewaters (ca. 6 - 9) were excluded (e.g. HSO_4^-, H_2SO_4, HF, HNO_3, HNO_2). The time derivative of the proton concentration is then[57]:

$$\frac{d[H^+]}{dt} = \left(\frac{d[TA]}{dt} - \sum_i \frac{\partial TA}{\partial X} \cdot \frac{d[X]}{dt} \right) \Big/ \frac{\partial [TA]}{d[H^+]} \quad (5)$$

where [X] is the concentration of the total acids that are pH-invariant. Each of the terms on the right-hand side of Eq. (5) is explicitly known, and their calculation is described by Hoffmann et al.[57]. The transport time derivatives of [X] are defined as sum of transport terms of the individual acid-base species, calculated from pH and the relevant stoichiometric equilibrium constants. Equilibrium constants and pH are defined on the free pH scale.

Sensitivity analysis

A two-level factorial analysis was used to determine the sensitivity of calcite dissolution on key boundary conditions (bottom water pH, O_2, T, S and POC rain rate). Factorial analysis is a statistical approach that monitors the response of a model output (e.g. a reaction rate or concentration) to the perturbations of n model factors, in this case the five variables listed above[59,60]. In a two-level analysis, each factor is assigned a high and low level based on the observations in nature. The procedure returns the effect of all possible factor permutations, that is, the change in model response between the low and high level. For n factors, there are a total of 2^n permutations and 2^n system responses, requiring 2^n model runs. A simplified version of the model was used in order to reduce the computational burden, and included organic carbon degradation, aerobic sulphide oxidation, anaerobic oxidation of methane and calcite dissolution (Supplementary Table 1). The latter was defined as:

$$R_{CaDiss} = f_T \cdot k_{CaDiss} \cdot CaCO_3 \cdot \left(1 - \Omega_{Calcite}\right)^{nc} \quad (6)$$

where k_{CaDiss} and nc were defined as 10 yr^{-1} and 4.7, respectively. Tested parameter ranges were 7.4 to 8.0 (pH), 5 to 340 µM (O_2), 5 to 35 (S) and 2 to 12 °C (T). The maximum level of the POC rain rate was set to the baseline value for Boknis Eck (12 mmol m^{-2} d^{-1}) since these sediments are highly reactive and receive large amounts of labile organic matter[20]. The minimum was set to 20% of this value. The mean rate of calcite dissolution at the end of a steady sate simulation was then noted. The results of these simulations are theoretical and do not necessarily reflect observations found in nature. The effects of the tested parameters are then determined using Yates' algorithm[60], including single parameter effects and effects arising from parameter interactions. The factors that have the largest impact on the system response can be visualized on a normal probability plot (Supplementary Fig. 5). The sensitivity analysis runs were executed without seasonality or artificial addition of calcite and therefore represent the long-term average situation (calcite rain rate = 3 mmol m^{-2} d^{-1}).

Estimating atmospheric CO_2 removal following carbonate addition in the Baltic Sea

The sediment model was used to provide an estimate of basin-wide atmospheric CO_2 drawdown after 10 years of continual mineral addition by running further simulations for representative areas of the Baltic Sea. We adopted the Baltic Sea sub-basins adopted by the BALTSEM model (Baltic Sea long-term large-scale eutrophication model)[27]. The thirteen regions in BALTSEM cover the entire Baltic Sea from the Kattegat in the west end to Bothnian Bay in the far north. Some of the smaller basins were combined for our analysis, to finally include the Kattegat (combining sub-basins 1-3), the Danish Straits (4-6), the Baltic Proper (7-9), Bothnian Sea (10), Bothnian Bay (11), Gulf of Riga (11) and Gulf of Finland (13). Data on mean physico-chemical properties of the water column (T, S, TA) for the year 2023 and for each sub-basin were extracted from BALTSEM (Table 2). These were employed as boundary conditions to run the sediment model for each region. Bottom water pH was calculated from TA and pCO_2, assuming equilibrium with the atmosphere (415 µatm). Dissolved O_2 was calculated using the T and S[61]. All other boundary conditions were taken from the Bothnian Bay simulation (Supplementary Table 5). We imposed a nominal 10% seasonal variability in bottom water pH, S, T, TA and O_2, using the same relative temporal changes as in the Boknis Eck model (Supplementary Fig. 1).

The benthic DIC and TA fluxes during 10 yr of artificial calcite addition determined with the sediment model for each sub-basin were recorded. The increase in DIC and TA fluxes after adding calcite (i.e. the fluxes due to calcite dissolution) were then imposed as input values to a 1-box model of the water column, again for each sub-basin. The box model assumes that the water column is well-mixed in the long-term, which is reasonable given the low mean water depths (Table 2). It is largely identical to a previous model for estimating the impact of olivine mineral dissolution on air-sea CO_2 fluxes[45]. This simple model does not consider lateral mixing between adjacent basins.

Total alkalinity and DIC in the water column model were defined as:

$$TA = [HCO_3^-] + 2[CO_3^{2-}] + [B(OH)_4^-] + [OH^-] - [H^+] \quad (7)$$

$$DIC = [CO_2] + [HCO_3^-] + [CO_3^{2-}] \quad (8)$$

Initial TA concentrations, along with S and T, were taken from BALTSEM (Table 2). As above, the initial pH was calculated from TA and CO_2 concentrations assuming equilibrium with the atmosphere and boric acid concentrations defined from salinity using appropriate equilibrium constants[51]. The model was run for 10 years where individual acid-base species were calculated at each time step.

CO_2 uptake from the atmosphere by the water column was calculated as:

$$FCO_2 = v_p \cdot ([CO_2]_{eq} - [CO_2]) \quad (9)$$

where v_P is the piston velocity (20 cm h^{-1} [41]), $[CO_2]_{eq}$ is the concentration of dissolved CO_2 at equilibrium with the atmosphere and $[CO_2]$ is the time-dependent concentration. FCO_2 represents the net CO_2 flux following mineral addition due to either direct uptake or a slow-down of outgassing. As defined, positive values denote CO_2 uptake from the atmosphere. The CO_2 uptake at the end of the simulation was upscaled for each basin by multiplying by the mud area of each box (Table 2).

The box model ignores key features of potential importance for CO_2 uptake, such as vertical and lateral mixing, spatially-resolved patterns of S and T, microalgae, as well as seasonal impacts on biology and carbonate system equilibria. The first-order estimate of CO_2 uptake in the Baltic Sea reported here provides an initial benchmark against which more robust estimates can be made based on fieldwork studies and coupled hydrodynamic-biogeochemical models.

Biogeochemical analyses

Sediments cores were sampled from Boknis Eck (~28 m water depth) between January 2022 and March 2023. Porewaters and solid phases were sub-sampled and analysed as described previously[20,21]. Measured data used to constrain the model are shown in Supplementary Fig. 2.

Data availability

Measured data used to constrain the model are available for download at https://doi.org/10.6084/m9.figshare.25932010.v1.

Code availability

Model code is available for download at https://doi.org/10.5281/zenodo.11501965. The code is written in MATHEMATICA v12 software (https://www.wolfram.com/mathematica/).

Received: 11 July 2023; Accepted: 11 July 2024;
Published online: 21 August 2024

References

1. IPCC (2018) Summary for Policymakers. In: Global Warming of 1.5 °C. An IPCC Special Report on the impacts of global warming of 1.5 °C above pre-industrial levels and related global greenhouse gas emission pathways, in the context of strengthening the global response to the threat of climate change, sustainable development, and efforts to eradicate poverty, Masson-Delmotte, V. et al. (eds.). Cambridge University Press, Cambridge, UK and New York, NY, USA, pp. 3−24. https://doi.org/10.1017/9781009157940.001.
2. Smith, S. M. et al. The State of Carbon Dioxide Removal - 1st Edition. Available at: https://www.stateofcdr.org (2023).
3. Oschlies, A. et al. Copernicus Publications, State Planet, 2-oae2023, https://doi.org/10.5194/sp-2-oae2023−1−2023 (2023).
4. Sabine, C. L. et al. The oceanic sink for anthropogenic CO2. *Science* **305**, 367–371 (2004).
5. Canadell, J. G. et. al. Global Carbon and other Biogeochemical Cycles and Feedbacks. In Climate Change 2021: The Physical Science Basis. Contribution of Working Group I to the Sixth Assessment Report of the Intergovernmental Panel on Climate Change [Masson-Delmotte, V., P. Zhai, A. Pirani, S. L. Connors, C. Péan, S. Berger, N. Caud, Y. Chen, L. Goldfarb, M. I. Gomis, M. Huang, K. Leitzell, E. Lonnoy, J. B. R. Matthews, T. K. Maycock, T. Waterfield, O. Yelekçi, R. Yu, and B. Zhou (eds.)]. Cambridge University Press, Cambridge, United Kingdom and New York, NY, USA, pp. 673–816, https://doi.org/10.1017/9781009157896.007 (2021).
6. Gattuso, J.-P. et al. Ocean Solutions to Address Climate Change and Its Effects on Marine Ecosystems. *Front. Mar. Sci.* **5**, 337 (2018).
7. Renforth, P. & Henderson, G. Assessing ocean alkalinity for carbon sequestration. *Rev. Geophys.* **55**, 636–674 (2017).
8. Eisaman, M. D. et al. Assessing the technical aspects of ocean-alkalinity-enhancement approaches, in: Guide to Best Practices in Ocean Alkalinity Enhancement Research, edited by: Oschlies, A., Stevenson, A., Bach, L. T., Fennel, K., Rickaby, R. E. M., Satterfield, T., Webb, R., & Gattuso, J. P., Copernicus Publications, State Planet, 2-oae2023, 3, https://doi.org/10.5194/sp-2-oae2023-3-2023 (2023).
9. Köhler, P., Abrams, J. F., Völker, C., Hauck, J. & Wolf-Gladrow, D. A. Geoengineering impact of open ocean dissolution of olivine on atmospheric CO2, surface ocean pH and marine biology, surface ocean pH and marine biology. *Environ. Res. Lett.* **8**, 014009 (2013).
10. Feng, E. Y., Koeve, W., Keller, D. P. & Oschlies, A. Model-based assessment of the CO2 sequestration potential of coastal ocean alkalinization. *Earth's Future* **5**, 1252–1266 (2017).
11. Fuhr, M. et al. Alkaline mineral addition to anoxic to hypoxic Baltic Sea sediments as a potentially effcient CO2-removal technique. *Front. Clim.* **6**, 1338556 (2024).
12. Krumins, V., Gehlen, M., Arndt, S., Van Cappellen, P. & Regnier, P. Dissolved inorganic carbon and alkalinity fluxes from coastal marine sediments: model estimates for different shelf environments and sensitivity to global change. *Biogeosciences* **10**, 371–398 (2013).
13. Meysman, F. J. R. & Montserrat, F. Negative CO_2 emissions via enhanced silicate weathering in coastal environments. *Biol. Lett.* **13**, 20160905 (2017).
14. Rao, A. M. F., Malkin, S. Y., Hidalgo-Martinez, S. & Meysman, F. J. R. The impact of electrogenic sulfide oxidation on elemental cycling and solute fluxes in coastal sediment. *Geochim. Cosmochim. Acta* **172**, 265–286 (2016).
15. Middelburg, J. J., Soetaert, K. & Hagens, M. Ocean alkalinity, buffering and biogeochemical processes. *Rev. Geophys.* **58**, e2019RG000681 (2020).
16. Melzner, F. et al. Future ocean acidification will be amplified by hypoxia in coastal habitats. *Mar. Biol.* **160**, 1875–1888 (2013).
17. Almroth-Rosell, E. et al. A Regime Shift Toward a More Anoxic Environment in a Eutrophic Sea in Northern Europe. *Front. Mar. Sci.* **8**, 799936 (2021).
18. Lennartz, S. T. et al. Long-term trends at the Boknis Eck time series station (Baltic Sea), 1957−2013: does climate change counteract the decline in eutrophication? *Biogeosciences* **11**, 6323–6339 (2014).
19. Balzer, W. Organic-matter degradation and biogenic element cycling in a nearshore sediment (Kiel-Bight). *Limnol. Oceanogr.* **29**, 1231–1246 (1984).
20. Dale, A. W., Bertics, V. J., Treude, T., Sommer, S. & Wallmann, K. Modeling benthic-pelagic nutrient exchange processes and porewater distributions in a seasonally hypoxic sediment: evidence for massive phosphate release by *Beggiatoa*? *Biogeosciences* **10**, 629–651 (2013).
21. Perner, M. et al. Environmental changes affect the microbial release of hydrogen sulfide and methane from sediments at Boknis Eck (SW Baltic Sea). *Front. Microbiol.* **13**, 1096062 (2022).
22. Wallmann, K. et al. Erosion of carbonate-bearing sedimentary rocks may close the alkalinity budget of the Baltic Sea and support atmospheric CO_2 uptake in coastal seas. *Front. Mar. Sci.* **9**, 968069 (2022).
23. Fehr, M. A., Andersson, P. S., Hålenius, U., Gustafsson, Ö., & Mörth, C. M. Iron enrichments and Fe isotopic compositions of surface sediments from the Gotland Deep, Baltic Sea. *Chem. Geol.* **277**, 310–322 (2010).
24. Retschko, A.-K., Vosteen, P., Plass, A., Welter, E. & Scholz, F. Comparison of sedimentary iron speciation obtained by sequential extraction and X-ray absorption spectroscopy. *Mar. Chem.* **252**, 104249 (2023).
25. Scholz, F., McManus, J. & Sommer, S. The manganese and iron shuttle in a modern euxinic basin and implications for molybdenum cycling at euxinic ocean margins. *Chem. Geol.* **355**, 56–68 (2013).

26. Lenz, C., Jilbert, T., Conley, D. J. & Slomp, C. P. Hypoxia driven variations in iron and manganese shuttling in the Baltic Sea over the past 8 kyr. *Geochem. Geophy. Geosy.* **16**, 3754–3766 (2015).
27. Gustafsson, E. et al. Sedimentary alkalinity generation and long-term alkalinity development in the Baltic Sea. *Biogeosciences* **16**, 437–456 (2019).
28. Meysman, F. J. R., Risgaard-Petersen, N., Malkin, S. Y. & Nielsen, L. P. The geochemical fingerprint of microbial long-distance electron transport in the seafloor. *Geochim. Cosmochim. Acta* **152**, 122–142 (2015).
29. Seitaj, D. et al. Cable bacteria generate a firewall against euxinia in seasonally hypoxic basins. *Proc. Nat. Acad. Sci. USA* **112**, 13278–13283 (2015).
30. Fuhr, M. et al. Disentangling artificial and natural benthic weathering in organic rich Baltic Sea sediments. *Front. Clim.* **5**, 1245580 (2023).
31. Flipkens, G. et al. Acute bioaccumulation and chronic toxicity of olivine in the marine amphipod Gammarus locusta. *Aquat. Toxicol.* **262**, 106662 (2023).
32. Oelkers, E. H., Declercq, J., Saldi, G. D., Gislason, S. R. & Schott, J. Olivine dissolution rates: A critical review. *Chem. Geol.* **500**, 1–19 (2018).
33. Leipe, T. et al. Particulate organic carbon (POC) in surface sediments of the Baltic Sea. *Geo-Mar. Lett.* **31**, 175–188 (2011).
34. Stockenberg, A. & Johnstone, R. W. Benthic denitrification in the Gulf of Bothnia. *Estuar. Coast. Shelf Sci.* **45**, 835–843 (1997).
35. Ulfsbo, A., Hulth, S. & Anderson, L. G. pH and biogeochemical processes in the Gotland Basin of the Baltic Sea. *Mar. Chem.* **127**, 20–30 (2011).
36. Sommer, S. et al. Major bottom water ventilation events do not significantly reduce basin-wide benthic N and P release in the Eastern Gotland Basin (Baltic Sea). *Front. Mar. Sci.* **4**, 18 (2017).
37. Soetaert, K. E. R., Hofmann, A. F., Middelburg, J. J., Meysman, F. J. R. & Greenwood, J. E. The effect of biogeochemical processes on pH. *Mar. Chem.* **105**, 30–51 (2007).
38. Dellwig, O. et al. Impact of the Major Baltic Inflow in 2014 on Manganese Cycling in the Gotland Deep (Baltic Sea). *Front. Mar. Sci.* **5**, 248 (2018).
39. Meier, H. E. M. Modeling the age of Baltic Seawater masses: Quantification and steady state sensitivity experiments. *J. Geophys. Res.* **110**, C02006 (2005).
40. He, J. & Tyka, M. D. Limits and CO_2 equilibration of near-coast alkalinity enhancement. *Biogeosciences* **20**, 27–43 (2023).
41. Gutiérrez-Loza, L. et al. Air–sea CO2 exchange in the Baltic Sea—A sensitivity analysis of the gas transfer velocity. *J. Mar. Sys.* **222**, 103603 (2021).
42. Fridahl, M. et al. Novel carbon dioxide removals techniques must be integrated into the European Union's climate policies. *Commun. Earth Environ.* **4**, 459 (2023).
43. Riebesell, U. et al. Copernicus Publications, State Planet, 2-oae2023, 6, https://doi.org/10.5194/sp-2-oae2023-6-2023.
44. Ho, D. T. et al. Copernicus Publications, State Planet, 2-oae2023, 12, https://doi.org/10.5194/sp-2-oae2023−12-2023.
45. Fuhr, M. et al. Kinetics of olivine weathering in seawater: An experimental study. *Front. Clim.* **4**, 831587 (2022).
46. Jahnke, R. A. The synthesis and solubility of carbonate fluorapatite. *Am. J. Sci.* **284**, 58–78 (1984).
47. HELCOM. State of the Baltic Sea – Second HELCOM holistic assessment 2011-2016. *Baltic Sea Environment Proceedings* 155 (2018).
48. Gustafsson, E. et al. Causes and consequences of acidification in the Baltic Sea: implications for monitoring and management. *Sci. Rep.* **13**, 16322 (2023).
49. Sayles, F. L., Martin, W. R., Chase, Z. & Anderson, R. F. Benthic remineralization and burial of biogenic SiO_2, $CaCO_3$, organic carbon, and detrital material in the Southern Ocean along a transect at 170° West. *Deep-Sea Res. II* **48**, 4323–4383 (2001).
50. Sulpis, O. et al. RADIv1: a non-steady-state early diagenetic model for ocean sediments in Julia and MATLAB/GNU Octave. *Geosci. Model Dev.* **15**, 2105–2131 (2022).
51. Zeebe, R. & Wolf-Gladrow, D. CO_2 in Seawater: Equilibrium, Kinetics and Isotopes, Elsevier, Amsterdam. ISBN: 9780444509468 (2001).
52. Mucci, A. The solubility of calcite and aragonite in seawater at various salinities, temperatures, and one atmosphere total pressure. *Am. J. Sci.* **283**, 780–799 (1983).
53. Subhas, A. V. et al. Catalysis and chemical mechanisms of calcite dissolution in seawater. *Proc. Natl. Acad. Sci. USA* **114**, 8175–8180 (2017).
54. Naviaux, J. D. et al. Calcite dissolution rates in seawater: Lab vs. in-situ measurements and inhibition by organic matter. *Mar. Chem.* **215**, 103684 (2019).
55. https://cdrmare.de/en. Last access 1 March 2024.
56. Montserrat, F. et al. Olivine Dissolution in Seawater: Implications for CO_2 Sequestration through Enhanced Weathering in Coastal *Environments*. *Environ. Sci. Technol.* **51**, 3960–3972 (2017).
57. Hofmann, A. F., Meysman, F. J. R., Soetaert, K. & Middelburg, J. J. A step-by-step procedure for pH model construction in aquatic systems. *Biogeosciences* **5**, 227–251 (2008).
58. Dickson, A. G. An exact definition of total alkalinity and a procedure for the estimation of alkalinity and total inorganic carbon from titration data. *Deep-Sea Res. A* **28**, 609–623 (1981).
59. Dale, A. W., Regnier, P. & Van Cappellen, P. Bioenergetic controls on anaerobic oxidation of methane (AOM) in coastal marine sediments: a theoretical analysis. *Am. J. Sci.* **306**, 246–294 (2006).
60. Box, G. E. P., Hunter, W. G., & Hunter, J. S. (1978) Statistics for experimenters. An introduction to design, data analysis and model building: New York, Wiley, 653 p.
61. Garcia, H. E. & Gordon, L. Oxygen solubility in seawater: better fitting equations. *Limnol. Oceanogr.* **37**, 1307–1312 (1992).

Acknowledgements

This work received funding by the German Federal Ministry of Education and Research, Grant No. 03F0895, Project RETAKE, DAM Mission "Marine carbon sinks in decarbonization pathways" (CDRmare). We thank Erik Gustafsson for providing data from the BALTSEM model. We are indebted to Subhadeep Rakshit (Dept. of Oceanography, Dalhousie University) for assistance with plotting the data using R software. We also thank Stefanie Böhnke-Brandt, Nicole Adam-Beyer, Gabriele Schüßler, Bettina Domeyer, Regina Surberg, Anke Bleyer and Anna-Kathrin Retschko for assistance during collection and analysis of sediment samples from Boknis Eck. The captain and crew of RV Littorina enabled easy-going sediment sampling in Boknis Eck. We are further grateful to Olivier Sulpis for editorial handling of our manuscript, and to Adam Subhas and the anonymous reviewers for their constructive comments.

Author contributions

A.W.D. and K.W. conceptualized the study, carried out the model simulations and prepared the manuscript. S.G. obtained funding and coordinated the project. M.F. advised on the modelling scenarios and interpretation of model results. M.P. coordinated the fieldwork and sediment sampling. I.D. and F.S. conducted geochemical measurements. All authors contributed, edited and commented on the manuscript.

Funding

Open Access funding enabled and organized by Projekt DEAL.

Competing interests

The authors declare no competing interest.

Additional information

Supplementary information The online version contains supplementary material available at https://doi.org/10.1038/s43247-024-01569-3.

Correspondence and requests for materials should be addressed to Andrew W. Dale.

Peer review information *Communications Earth & Environment* thanks Adam Subhas and the other, anonymous, reviewer(s) for their contribution to the peer review of this work. Primary Handling Editors: Olivier Sulpis, Clare Davis, and Carolina Ortiz Guerrero. A peer review file is available.